JOURNAL OF MATERIALS SCIENCE: MATERIALS IN MEDICINE **16** (2005) 301 – 312

Characterization of surface modified Ti-6Al-7Nb alloy

S. SPRIANO[1,*], M. BRONZONI[1], E. VERNÈ[1], G. MAINA[2], V. BERGO[2], M. WINDLER[3]
[1]*Material Science and Chemical Engineering Department, Politecnico di Torino, Italy*
E-mail: silvia.spriano@polito.it
[2]*Traumatology Orthopaedics and Occupational Medicine Department, University of Turin, Italy*
[3]*Zimmer, Inc, Warsaw, Poland*

In the last years different types of surface modifications were developed with the aim of improving the osteointegration ability of titanium alloys. The chemical composition, crystallographic structure and morphology of a surface layer can be modified in order to obtain a better interaction between the implant, the cells and the organic fluids. The final goal is to obtain a more efficient bone growth also in critical clinical cases. In the present paper were reported several data about the characterization of the Ti-6Al-7Nb alloy treated by two innovative surface treatments. They consist of blasting, followed by a two step chemical etching and heat treatment performed in air or in vacuum. TEM, XRD and SEM investigations were performed in order to assess the structure and morphology of the modified surfaces. The surface chemical composition was investigated by XPS ad AES analyses. The ability to interact with physiological fluids was tested by immersion of the treated materials in an acellular simulated body fluid (SBF). Metal ion concentration analyses of the fluid and SEM observations of the samples were performed after different times of soaking. The mechanical characterization involved scratch and fatigue tests.

The surface of treated samples shows chemical, structural and morphological modifications. The passivation pre-treatment has influence on the surface modification. The treated samples evidenced a quite low metal ion release and interact with SBF solution, showing a moderate bioactivity. A relevant decrease in fatigue strength was observed on modified samples.

1. Introduction

New thermo-chemical treatments were conceived in order to obtain titanium alloy implants presenting better osteointegration ability. The present paper describes the characterization of treated Ti-6Al-7Nb alloy samples, with the aim of comparing literature treatments and the new ones and optimizing the effectiveness of the latter.

Despite of the good performances of titanium prostheses, the native titanium oxide does not allow adequate osteointegration when a low quality bone bed is present or when faster healing is required. At this regard metal implants presenting a bioactive behaviour are of great interest, according to their ability of stimulating bone growth. A first generation of these implants included titanium alloys coated by hydroxylapatite. In order to avoid disadvantages of plasma-spray coating, it could be advantageous to modify the surface by using thermochemical treatments. So a second kind of bioactive metal implants is under inspection, which includes chemical and heat-treated titanium alloys, presenting the ability of inducing the precipitation of hydroxylapatite and bone growth after implantation. Considering that implant-bone interaction is quite a complex event [1, 2] depending first of all on several features of the implant surface, as its chemical composition, wettability, presence of crystalline and/or amorphous phases, roughness and porosity, as well as bone cell and bone interaction, a detailed characterisation of the modified surfaces was performed.

The first step of the new processes proposed involves grit blasting of the surfaces. It was selected according to better performance of rough surfaces respect to osteointegration ability and mechanical adhesion to bone. It must be considered that the surface properties of blasted titanium alloys are not completely analogous to those of grinded or electropolished ones, because of chemical modifications due to mechanical damage [3]. So their properties and behaviour were investigated in a specified way and the mechanical treatment of the surface must be considered as part of the processes. The

*Author to whom all correspondence should be addressed.

chemical treatment of the specimens represents the next step. It involves both acid and alkali etching with the aim of obtaining a microporous modified surface layer. Different NaOH molar solutions were tested in order to evaluate the effect of alkali solution concentration on surface modification. The last step consists in a heat treatment, performed in air or in vacuum, in order to increase the mechanical adhesion of the surface layer. The heat treatment in vacuum was considered also in order to obtain better fatigue properties [4].

The crystallographic structure of the treated samples was assessed by Transmission Electron Microscopy (TEM) and X-ray Diffraction analysis (XRD). The surface morphology was investigated by Scanning Electron Microscopy (SEM) and its composition was evaluated by Energy Dispersion Spectroscopy (EDS), X-ray Photoelectron Spectroscopy (XPS) and Auger Electron Spectroscopy (AES). Moreover, in order to verify the bioactive behaviour of the treated alloy, in-vitro tests were performed by soaking samples in simulated body fluid and the new process was compared with other thermochemical treatments proposed in literature [5, 6]. A relevant question was to assess the corrosion resistance of the treated implants and their possible metal ion release, so metal ion concentration analyses, after soaking in acellular simulated body fluid (SBF), were performed by absorption spectrophotometry (GFAA-ICP). The mechanical adhesion of the surface layers to the metallic substrate was tested by scratch tests. Fatigue tests were also performed in order to give a complete characterisation of the treated materials.

2. Experimental

For the present research work the Ti-6Al-7Nb alloy was employed and all experiments were carried out on 18 mm diameter, 2 mm thick disks supplied by Centerpulse Orthopaedics (now Zimmer, Inc). The blasted samples were prepared by Centerpulse Orthopaedics by grit blasting with corundum. The roughness of the disks was Ra $\cong$ 4–6 μm. The mechanically polished samples were prepared by using a 1 μm diamond abrasive paste as last finish.

The acronyms used to identify the different chemical and heat treatments are reported in Table I. The ML and BL samples correspond to mirror polished and sandblasted specimens treated by the chemical and heat treatment proposed in literature [5]. BPAA and BPAV treatments correspond to the new processes proposed. They consist of two chemical steps (passivation and alkali etching) and an air/vacuum heat treatment. The passivation was performed in 35–40 wt% HNO_3, at room temperature, for 30 min. The alkali etching was performed in 2–10 M NaOH, at 60 °C, for 24 h. All the samples were washed with distilled water and dried at room temperature after acid and alkali etching. The air heat treatment was performed by dwelling the samples at 600 °C for 1 h in a standard electric furnace. The heating rate employed was 300 °C/h as well as the initial cooling rate. The vacuum heat treatment was performed under rotative pump dynamic vacuum conditions (5×10^{-1} mbar). After heat treatment the specimens were washed with acetone and dried at room temperature.

Surface crystalline structure was investigated by X-ray diffraction analysis (X'Pert Philips diffractometer), using the parallel beam camera geometry (XRD-PB) and the Cu-K_α incident radiation. The incident angle was set at 1.2 degrees.

TEM investigation was performed by using a Philips CM12 electron microscope, operated at 120 kV. Ti grids were treated according to the processes described and used as samples. TEM camera diffraction constant was assessed on a pure Al standard sample.

Surface morphology and composition were assessed by scanning electron microscopy (SEM Philips 525 M) and energy dispersion spectrometry (EDS Philips—EDAX 9100).

Metal ion release measurements were performed by soaking disk-shaped samples in standard Simulated Body Fluid solution (SBF) maintained at 37 °C [7]. Small amounts of solution were withdrawn at different times, ranging from 3 h to 60 days, and replaced with fresh solution. An atomic absorption spectrophotometer (GFAA-ICP technique) was used to evaluate metal ions concentration in the withdrawn solution, focusing on titanium and aluminium content. For every different treatment tests were carried out on at least 3 samples. Replacing the withdrawn solution with fresh one leads to dilution effects. Knowing exactly the amount of soaking solution and the withdrawn (and replaced) quantity it was possible to process the data taking into account the experimental procedure.

TABLE I Sample acronyms legend

	Mechanical polishing	Blasting	Passivation	Alkali etching	Air heat-treatment	Vacuum heat treatment
ML	X			X (5 M)	X	
BL		X		X (5 M)	X	
BP		X	X			
BPA		X	X	X (5 M)		
BPAA		X	X	X (5 M)	X	
BPAV		X	X	X (5 M)		X
MPAA	X		X	X (5 M)	X	
MPAV	X		X	X (5 M)		X
MPA	X		X	X (5 M)		
BPAA-2 M		X	X	X (2 M)	X	
BPAA-7 M		X	X	X(7 M)	X	
BPAA-10 M		X	X	X (10 M)	X	

Scratch tests were carried out in order to evaluate the adhesion of the surface reaction layers to the substrate depending on the different treatments. The tests were performed by using a Rockwell C indenter, with a diamond tip radius of 0.2 mm. Two scratches were made on each sample at the constant rate of 10 mm/min and by increasing the load at 10 or 100 N/min in the range of 1–50 N or 1–10 N. The most relevant results were obtained by comparing the scratches performed at 100 N/min, so in the following only these data will be reported. Images of the scratch lines left on the surface were later taken with SEM. Samples were mechanically polished (mirror finish) prior to the various treatments, in order to have a regular surface with plain layers grown on it.

Auger Electron Spectroscopy (AES) was carried out in order to have more information on chemical composition as a function of the distance from the upper surface of the treated samples, collecting data on the thickness of the reaction layer and on the diffusion of oxygen. Auger Electron Spectroscopy (AES) analysis was performed by using a VG-LEG200 instrument. The measurements were performed by applying a current beam of 0.1 A and measuring a current of 1.3 μA on an area of 6 mm^2. During the Ar^+ sputtering a spectrum was acquired every 30 s.

XPS analyses were also performed in order to investigate the Na/Ti atomic ratio, since Na signal was difficult to detect by AES . XPS spectra were collected by using a VG Escalab 200-C spectrometer equipped with a hemispheric analyzer at 5 channeltron. Two non monochromatic X radiations were employed, corresponding to AlKa ($E = 1486.6$ eV, $W = 0.85$ eV) and MgKa ($E = 1253.6$ eV, $W = 0.8$ eV). The instrument works at a vacuum value of 5×10^{-9} mbar. The Na/Ti atomic ratio was calculated measuring the area related to Na 1s e Ti 2p peaks registered by using the MgKa radiation ($\Delta E = 0 \div 1100$ eV, Energy resolution = 1.70 eV, step = 0.8). The values were normalized by considering the transmission factor and the impact section.

Mechanical fatigue tests were carried out in order to evaluate the effect of the proposed thermo-chemical treatments on fatigue resistance. At least seven samples for each proposed treatment, plus fifteen untreated reference samples, were tested in a high cycle rotation beam fatigue machine. The test conditions were: 100 Hertz for 10 million cycles in air at room temperature and stress ration $R = -1$. All specimens had a gauge diameter of 4 mm. Due to low sample numbers, the fatigue limit could not be calculated with statistic analysis. The fatigue limit is defined as the level where no fracture occurred during testing.

3. Results

3.1. Surface morphology (SEM observations)

No evident modification in morphology or composition of the surface was detected after passivation in HNO_3 alone (BP samples).

The presence of a microporous layer was observed on the passivated and NaOH treated samples, analysed before heat treatment. The average diameter of the micropores is about 0.1 μm. A hardly detectable Na signal resulted from EDS analysis on the alkali treated samples, but it was too weak in order to perform a detailed investigation by means of this technique. The heat treatment at 600 °C caused a densification of the porous surface, and the growth of a homogeneous layer consisting of almost spherical and thickened particles can be observed. They are about 80 nm in diameter. In case of a previous passivation treatment there is no modification of the surface morphology, and no significant differences were detected between air and vacuum treated samples. Fig. 1(a) shows the surface of a BPAV sample. No evident compositional changes were evidenced by means of EDS after any heat treatments.

Different alkali solution concentrations were tested in order to identify the best experimental condition of the process. The best NaOH concentration to be used was assessed to be 5 M [5]. With such concentration a continuous and adherent layer was obtained (see Fig. 1(b), showing a BPAA sample). On the contrary a more aggressive solution (10 M) produced a surface layer presenting deep cracks on it both before and after heat treatment (Fig. 1(c) shows a BPAA-10 M treated sample). The morphology of the surface layer of BPAA-10 M treated samples was quite alike to the 5 M ones; just a slight increase in the spherical particles dimension could be registered (100 nm). Some cracks were also observed by using 7 M NaOH (Fig. 1(d)—BPAA-7 M). 2 M NaOH solution was also tested (BPAA-2M sample) as etching solution: in this case a crack free surface layer was obtained, but the 5 M one was selected as preferable considering the need for a thicker surface layer. So in the following the NaOH concentration employed must be considered as 5 M, unless different labels reported.

3.2. Crystallographic structure analysis (XRD, TEM)

No relevant diffraction peaks, apart from those due to the substrate, were detected on BP samples.

The XRD patterns obtained for BPA, BPAA, BPAV and BL samples are reported on Fig. 2. It can be noticed that a diffraction signal at about $2\theta = 25.5°$ was registered on all the treated samples. A second signal, centred at about $2\theta = 27.5°$ was observed only on the air heat-treated samples (BL, BPAA). The others signals were ascribed to the titanium substrate.

The first signal could be assigned to a titanium oxide, as well as brookite, anatase or Ti_3O_5 monoclinic phase or to a sodium-containing titanium oxide, as for instance $Na_2Ti_3O_7$. According to the reduced thickness of the surface layer and to the difficulty to detect it by XRD, even by using parallel beam configuration, the awarding of the first diffraction peak to a unique phase is quite dubious. On the other hand it is easier to ascribe the second signal to rutile. By comparing these data with diffraction patterns reported in literature [8–10] a substantial agreement can be observed apart from the awarding of the first peak to a sodium titanate phase that needs to be confirmed by other techniques.

In order to investigate in detail the crystallographic structure and the microstructure of the treated samples, TEM observations on unalloyed titanium grids were

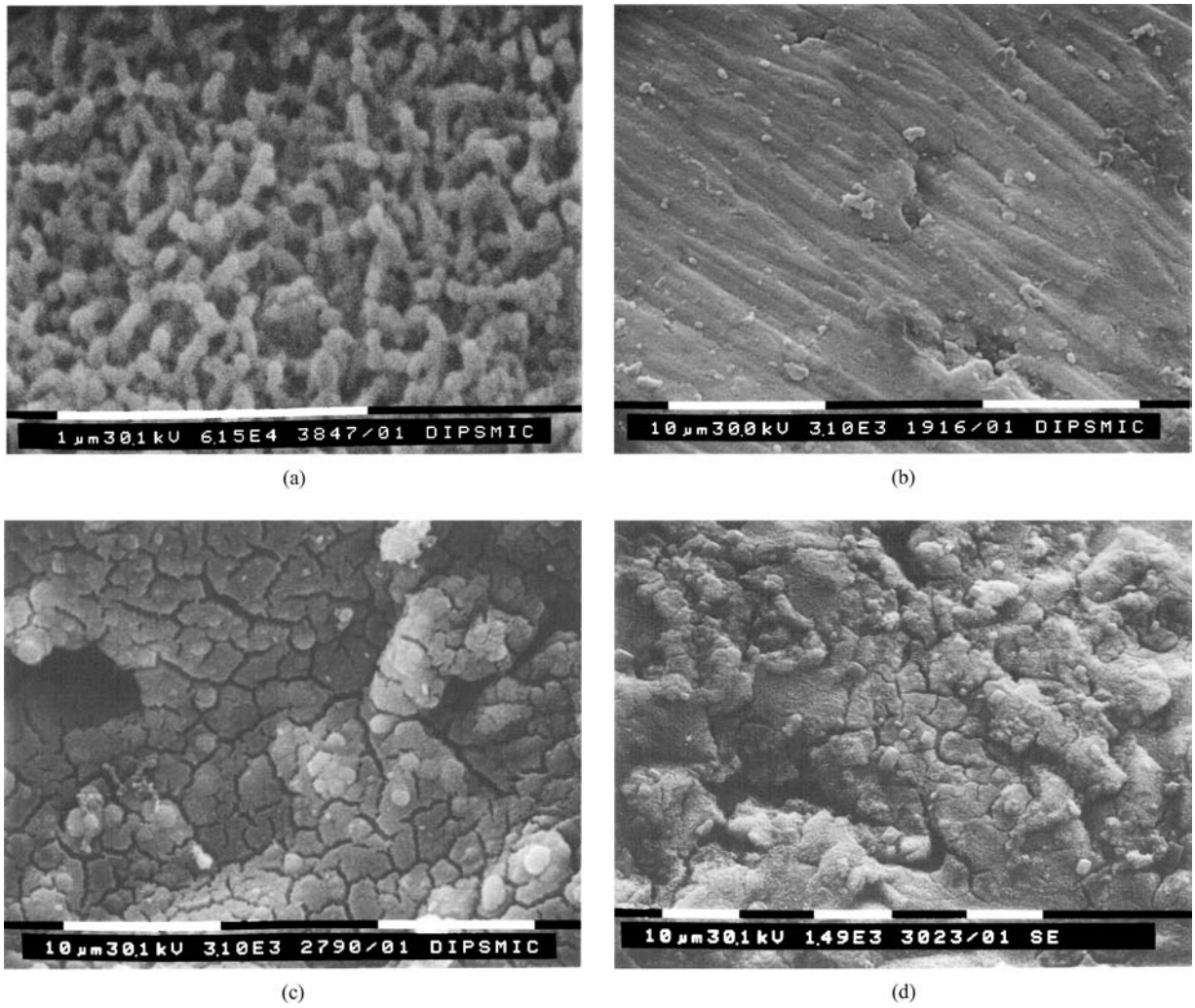

Figure 1 SEM images showing the morphology of (a) BPAV, (b) BPAA, (c) BPAA-10 M, and (d) BPAA-7 M samples.

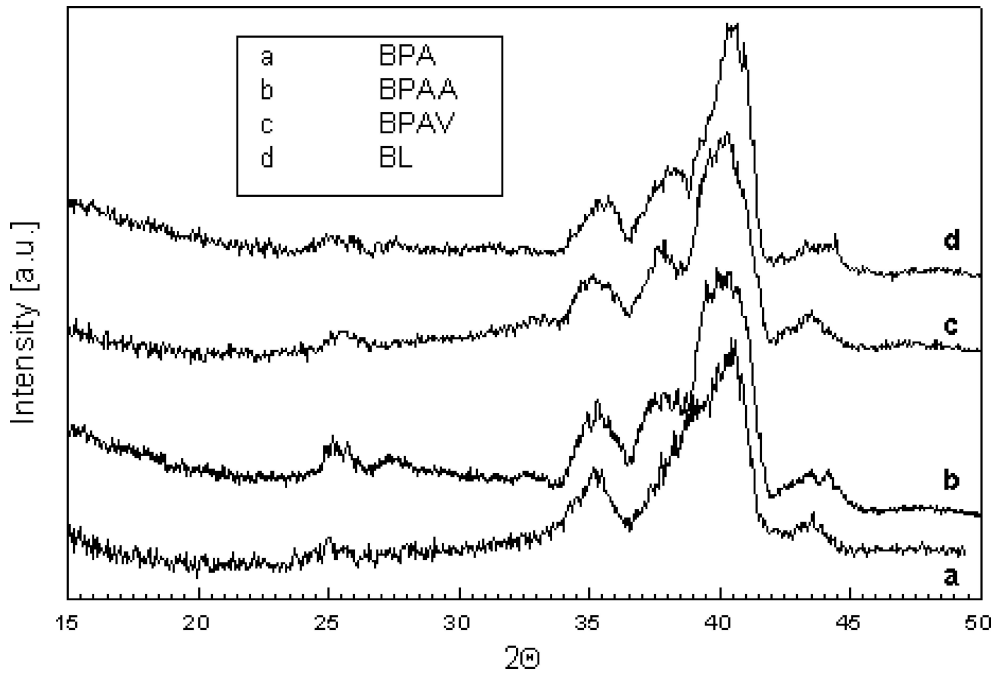

Figure 2 Parallel-beam XRD diffraction patterns of samples with different treatments (see Table I for acronyms).

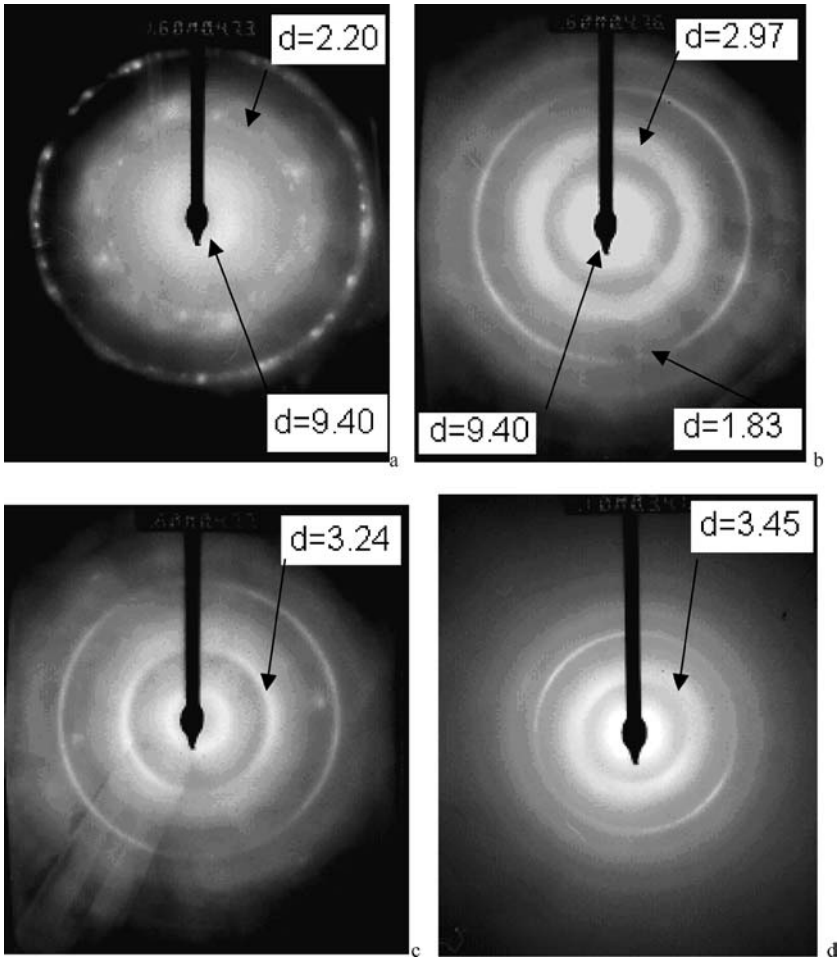

Figure 3 SAD pattern of a (a) NaOH 5 M etched sample, (b) passivated + NaOH etched sample, (c) passivated + NaOH etched + air heat-treated sample, (d) passivated + NaOH etched + vacuum heat-treated + 30-day SBF soaked sample. Samples consist of TEM Ti grids.

performed. This method was preferred respect to the stripping of the surface layers from the substrate in order to avoid any artificial effect due to sample preparation. Obviously these data will be evaluated considering differences of the chemical composition of the starting material and of the mechanical state of these samples, respect to the others materials employed during this research activity.

The passivation treatment alone did not modify the bright field image of the sample. So it can be deduced that the surface layer was quite thin, smooth and adherent to the titanium substrate. The electron diffraction pattern showed the Ti spots as well as some weak signals due to Ti_3O_5 monoclinic phase.

The electron diffraction pattern of the NaOH treated sample is reported in Fig. 3(a). Apart from Ti diffraction spots, a broad halo, centred at about $d = 2.20$ Å, due to an amorphous phase (it will be called α amorphous phase) can be observed. A ring quite close to the transmitted beam spot corresponding to $d = 9.4$ Å was also detected and it can be assigned to the Ti_3O_5 monoclinic phase. On the contrary the electron diffraction pattern shows different signals (Fig. 3(b)) when both acid and alkali chemical treatments are performed. A broad halo is still observable, but it is now centred at about $d = 2.97$ Å (β amorphous phase) and two rings corresponding to $d = 1.83$ Å and $d = 9.4$ Å can be observed. The first ring can be ascribed to anatase, whose main signal is covered by the amorphous halo, and the last one to Ti_3O_5. The morphology of the crystals in the sample after alkali etching is reported in Fig. 4(a) and (b). The sample is covered by a sort of uniform and continuous threadlike layer overhanging the grit. The bright field image of the sample does not substantially change when performing nitric passivation before alkali etching. The microphotograph shows the quite fine scale of the microstructure. Because of their small dimensions, crystals could not be marked out from the amorphous matrix they were embedded in.

The passivated, alkali etched and vacuum heat-treated sample looks quite alike to the sample before heat treatment, both by considering bright field image and electron diffraction pattern. So it can be concluded that vacuum heat treatment does not modify substantially the structure and microstructure of the sample.

The last sample analysed is a passivated, alkali etched and air heat-treated sample. It is quite similar to the previous one by considering bright field image, while the diffraction pattern shows an intense ring corresponding to $d = 3.24$ Å superimposed on the β-amorphous halo and attributed to rutile (Fig. 3(c)). The amorphous halo is still detectable, but it is less bright and uniform then in the previous case. So it can be concluded that the air heat-treatment induces a relevant crystallisation of the sample with the formation of the rutile phase.

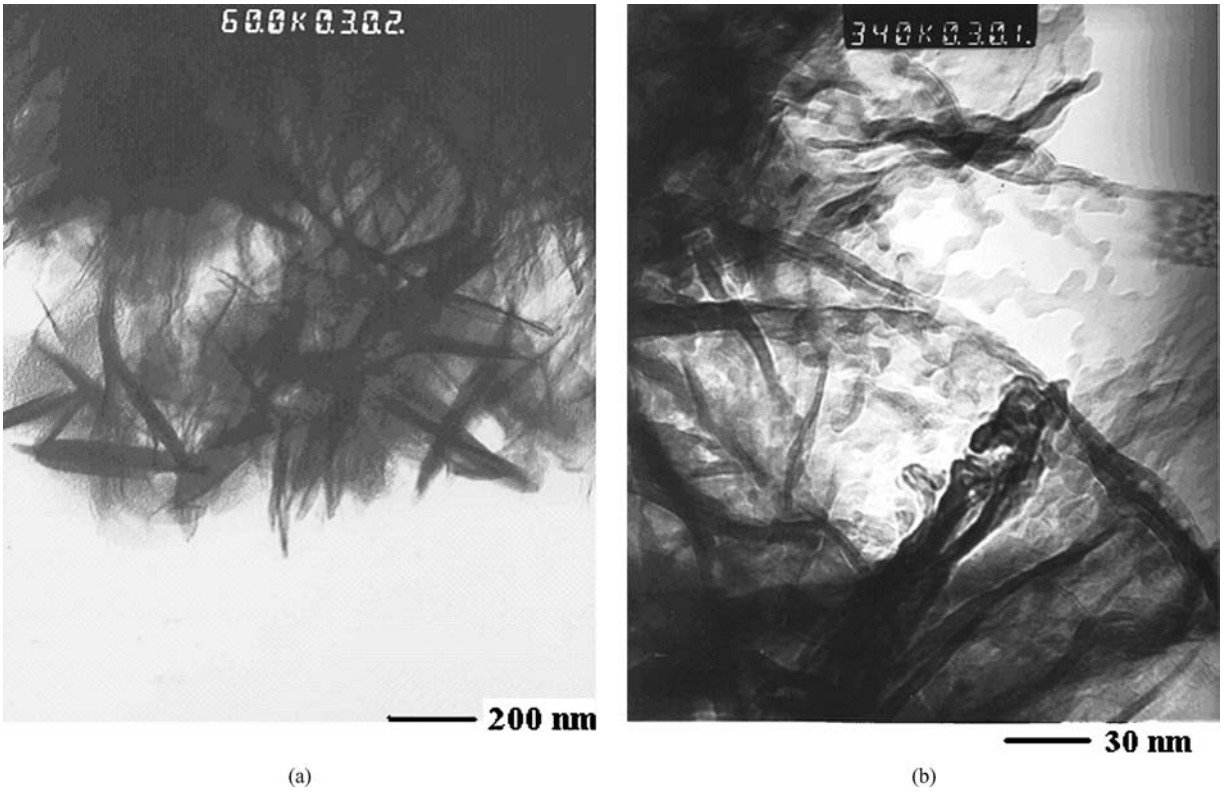

Figure 4 (a)–(b) Bright field TEM images of an alkali etched sample, showing the morphology of the crystals at different magnification. (c) Bright field TEM images of a passivated, alkali etched and vacuum heat-treated sample after 30 days of soaking in SBF, showing the morphology of the crystals.

The TEM microscope was equipped by an EDS analyser and the compositional analysis evidenced a weak signal related to Na only on the NaOH treated sample (without passivation and heat treatment), while on all the other samples it was absent. So, by considering TEM-EDS data, the presence of a titanate phase on the treated samples can be excluded.

After soaking in SBF for 30 days, morphology, structure and composition of the treated titanium grits are different, confirming the material ability to interact with the physiologic liquids. In the cases of the passivated, alkali etched and vacuum heat-treated sample, an amorphous halo centred at about 3.45 Å can be observed (γ amorphous phase) (Fig. 3(d)). It must be considered that crystalline apatite shows an intense diffraction peak close to this position. EDS analysis showed the presence of Ca and P and the morphology of the sample presented small rounded crystals (Fig. 4(c)). These data were interpreted by considering the growth on the sample of an amorphous phase that could represent a precursor of apatite crystals [10–12]. Also the passivated, alkali etched and air heat-treated sample showed evidence of morphology and structure changing after 30 days soaking in SBF, but they were less marked than in the previous case.

Several differences can be evidenced between our data and TEM analysis reported in literature about alkali etched and air heat-treated samples [13]. We could not observe the presence of a strong Na signal on EDS analysis, reported by some authors. Furthermore only the presence of rutile and titanate as crystalline phases was evidenced.

3.3. Surface chemical composition analysis (AES, XPS)

AES depth profiles of the surfaces of BP, BPA, BPAA, BPAV and ML samples are reported in Fig. 5. In the case of ML samples the surface was grinded by using a 600-grit paper before chemical and thermal treatment, as suggested in literature [5]. Due to experimental difficulties occurred acquiring the AES spectra on rough surfaces, Nb and Na signals were very noisy, and they were not reported on the graphics. So on the y-axis an arbitrary unit instead of atomic concentration is used.

In the case of the blasted and passivated sample (BP) the surface oxide is quite thin and a rapid increase of the Ti level and specular decrease of O content occurs just below the surface (Fig. 5(a)).

In the case of the blasted, passivated and alkali-etched surface (BPA) a thicker oxide layer can be noted (Fig. 5(b)). The Ti and O concentration presents a plateau followed by an increase/decrease of the Ti/O content. The presence of a net interface between the surface oxide and the bulk is not evident, but a border region can be found after a time sputtering of about 600 s. On the air heat-treated (BPAA) sample no interface can be detected and both Ti and O contents increase/decrease in a quite smooth and gradual way (Fig. 5(c)). By using the intersection between Ti and O depth profile curves as reference it can be underlined that this sample presents the thickest surface oxide. Titanium and oxygen depth profiles are also rather smooth in the case of vacuum heat-treated sample (BPAV-Fig. 5(d)), but in this case the oxide layer is thinner than on the air-treated sample. On the contrary in the

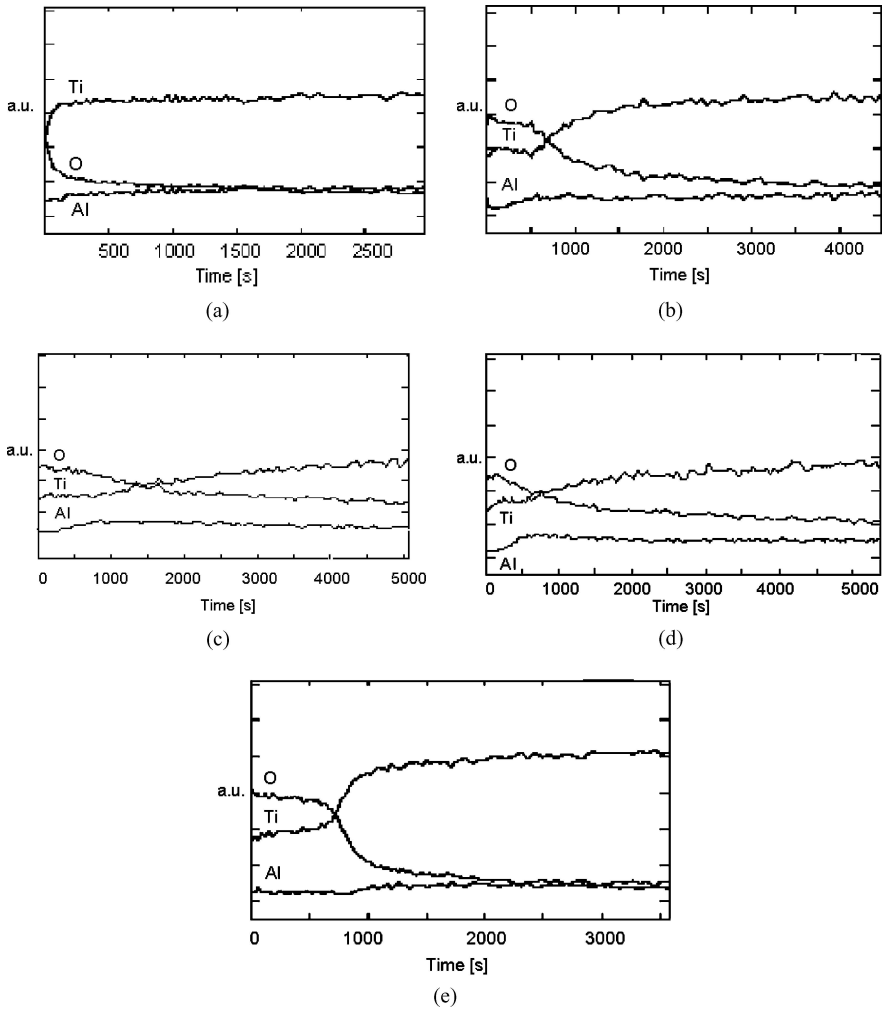

Figure 5 Auger depth profiles of samples with different treatments (see Table I for acronyms): (a) BP, (b) BPA, (c) BPAA, (d) BPAV, (e) ML (literature process).

case of the sample treated according to the literature treatment (ML) the depth profile shows an abrupt Ti increase and specular O decrease (Fig. 5(e)). In this case a net interface between the surface and the deeper region can be identified at about 800 s as time sputtering.

On all samples the Al level shows a slight increase moving from the surface towards the bulk. The Na signal was quite noisy for all samples and difficult to be detected. For BPA, BPAA, BPAV and ML samples, that is for all the alkali treated samples, it was slightly higher on the surface respect to the bulk, but its trend was not clear. So XPS analysis was also performed. The Ti/Na atomic ratio registered on the BPA, BPAA, BPAV and ML samples were respectively 0.3, 1.0, 0.6, 0.4. These data can not be used as quantitative information, but it can be qualitatively concluded that Na is present on the surface of treated samples. Its presence is limited just to the external layer and abruptly decreases moving to the deeper region.

AES data reported in literature [9, 14, 15] are substantially in agreement with our results on ML sample. It can be observed by these literature data that NaOH treated samples, without passivation pre-treatment, present a net interface between the surface and the deeper region with a more marked concentration gradient respect to our data on passivated and alkali etched sample (BPA).

3.4. Mechanical testing (scratch and fatigue test)

Scratch tests were performed on mirror polished samples submitted to different treatments, with the aim of comparing the mechanical behaviour and adhesion to the substrate of the different surface layers. This technique can not be applied to blasted and rough surfaces, so smooth samples were prepared. MPA, MPAA, ML and MPAV treatments were chosen.

A critical load can not be registered by the acoustical emission detector during all the tests, so it can be deduced that the surface layer deadhesion is not a catastrophic event of brittle nature. Comparisons among different samples were performed by SEM observations of the scratch line morphology.

The starting and the end of the scratch lines were observed by SEM. On the ML sample an irregular ridges shape starts from 0.23 mm (that means up to a load of about 2.3 N). In the case of MPAV the first 0.65 mm (corresponding to 6.5 N) of the scratch line show a smooth appearance of the scratch edges and bottom, without evidence of damage and of irregular ridges. On the MPAA sample the first damage evidence (irregular ridges and removed particles) appears at 1.0 mm (10 N), and on the MPA sample 1.5 mm (15 N).

By observing the last part of the scratch it was underlined that in the case of MPAV sample the scratch

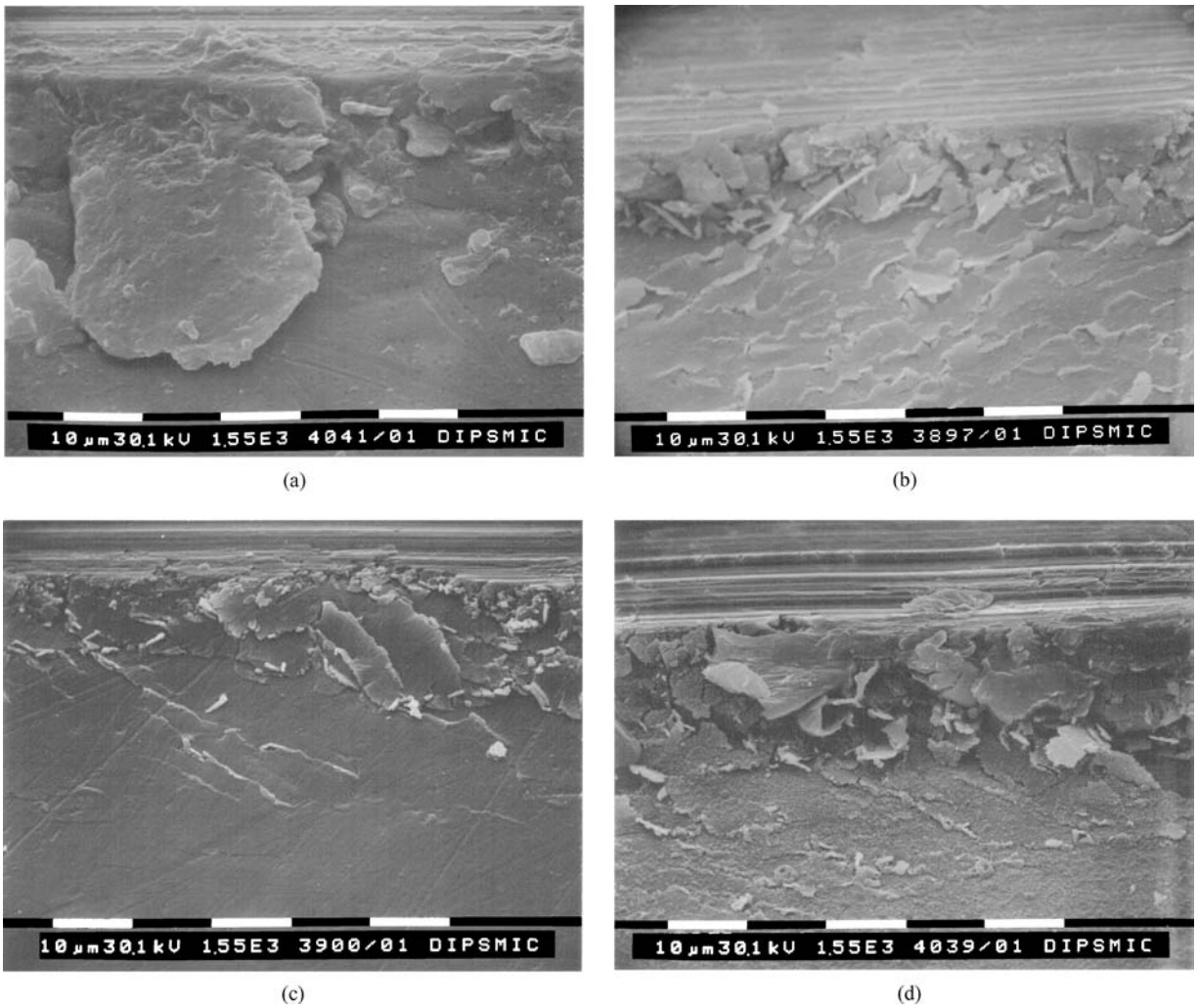

Figure 6 End parts of scratch lines on (a) MPA, (b) MPAA, (c) MPAV, (d) ML samples.

shows the smoothest and least damaged aspect, while the MPA sample presents the softest behaviour with big chips and removed particles. Cracks are evidenced on the bottom of the ML sample.

A zoom of the end side of the scratches is reported in Fig. 6(a)–(d). The low damage and crack initiation of the MPAV sample is confirmed. On the contrary a relevant amount of removed material by the indenter in the case of ML sample becomes evident. The MPA sample confirms its soft and ductile behaviour without crack presence on the ridges.

A correct comparison with literature data about adhesion of titanium coating presenting good osteointegrability, as for example plasma sprayed hydroxylapatite, can not be performed because of slight differences in experimental parameters, as the shape of the indenter of the rate of loading. In any case a brittle decohesion of the coating at a load between 0.4 and 5.7 N is reported by different authors [16–19]. So the behaviour of the surface layers investigated during this experimental research seems to be comparable or better.

The fatigue strength (where no fracture occurred) was for either chemical or heat- treated series 260 MPa. No influence of the heat treatment medium, air vs. vacuum could be detected. The fatigue strength of the grit blasted series without any additional treatment was 460 MPa and therefore significantly higher. All fatigue fractures initiated at the surface.

3.5. Metal ion release analysis (GFAA-ICP data)

Metal ion concentration analyses were performed on acellular simulated body fluid (SBF), after soaking of the different samples for one month in it. Our experiments were carried out on Ti-6Al-7Nb samples with a sandblasted surface. They were aimed to compare the behaviour of samples treated by passivation alone (BP) or by the new treatment (BPAA) with different alkali etching solution concentrations (BPAA, BPAA-10 M), to literature data. All data regarding Al ion release tests are reported in Fig. 7.

As shown in the diagram, all kinds of samples induce a rapid increase in Al ion concentration during the first 3 days. After longer time exposures, the SBF shows a slowly increasing concentration of metal ions.

As reference it can be considered that samples that were only passivated with HNO_3 induced a concentration of 7 μg/L for Al ions after 28 days. With samples treated according to the new process, we obtained after the same soaking time, about 6 μg/L for Al ions. The new process was also tested with a different concentration of the alkaline etching solution, 10 M instead

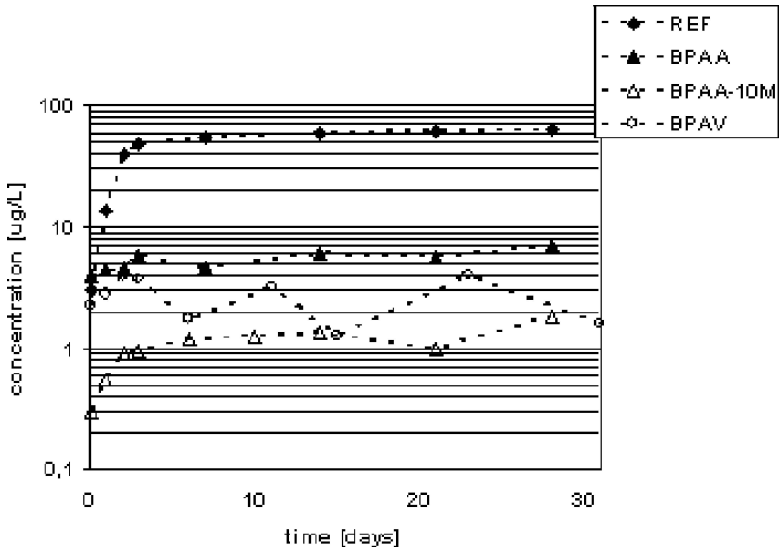

Figure 7 Al ion concentration in SBF after soaking of treated samples for various times. REF indicates literature data for BL samples.

of the standard value of 5 M: in this case we obtained about 2 μg/L as maximum value for Al ion release.

Values for Ti ions were negligible in all cases, except for BPAA-10 M samples: in that case, we obtained about 2 μg/L after 28 days as soaking time.

Literature data [8] refer to Ti-6Al-2Nb-Ta samples with a grinded surface, treated by alkali etching and air heat treatment. Al ion concentration reaches more than 50 μg/L after 28 days, while values for Ti ions are negligible.

Our values for Al ions release are about one order of magnitude lower than literature ones, so the passivation stage introduced by the new process seems to be effective against Al ions release. The passivation alone seems to be effective as well, but electrochemical tests [20] have demonstrated that only BPAA samples have good corrosion behaviour also in aggressive environments. About Al ion release, values for BPAA-10 M samples are even better than those for BPAA samples, but Ti ion release data must be also taken into account.

In the case of BPAA and BPAV metal ion release measurements after two months as soaking time were also performed in order to confirm that a plateau value was reached. Al ion concentration is again under 10 μg/L even after 2 months and Ti ion concentration reaches a maximum of 2 μg/L in both cases.

4. Discussion

The main objective of the research project was to investigate alternative processes, respect to plasma sprayed hydroxylapatite (HA) coating, in order to obtain metallic biomaterials presenting good osteointegrability. In fact plasma spray is an expensive technique and many authors have reported that plasma sprayed HA coatings enhanced implant performance at an early stage after implantation, but caused poorer long-term performances because of low adhesion of the coating to the metal and low crystallinity of the HA. Furthermore it is difficult to obtain uniform and thin coating on implants with a complex shape [21, 22].

In the present work two thermochemical treatments were tested in order to modify the surface of Ti-6Al-7Nb alloy, with the aim of obtaining better osteointegration ability. They consist of blasting, passivation in nitric acid solution, alkali etching in NaOH solution and air (BPAA) or vacuum (BPAV) heat treatment at 600 °C for 1 h.

The main data obtained by the present characterization of the modified surfaces can be summarised as follows.

By comparing the effects of different alkali etching solutions (2-5-7-10 M NaOH) on the morphology of the surface layer, it can be concluded that the best results were obtained by using a 5 M solution. In this case a surface free from cracks was observed, presenting a macroscopic roughness due to blasting and a small-scale porosity (80 nm) due to the chemical etching.

By observing the XRD data, it can be concluded that the alkali etching of the alloy, or of its passivated surface, produces a structural modification that is retained after heat treatment. The air heat treatment involves rutile formation while the vacuum heat treatment does not. Moreover TEM data suggest that the passivation pre-treatment causes the formation of different crystallographic phases (a different amorphous phase and the appearance of anatase crystals). The samples treated by the proposed innovative processes interact with the simulated physiological solution, showing a moderate bioactivity and the formation of apatite amorphous precursor by soaking in SBF. No evidence of titanate phase was found and the Na presence seams to be limited to a quite thin surface layer (XPS data), thinner than the surface oxide due to the thermochemical treatment.

The bioactive behaviour of treated titanium or titanium alloys surfaces was rather widely treated in literature during the last 6–7 years [5], but its mechanism as well as the relevance of the surface morphology and composition, as well as crystallographic phases involved is still a discussed topic. Some authors reported in several papers [5, 10, 23] the formation of hydroxylapatite on NaOH etched surfaces during soaking in SBF and described the bioactive behaviour as an ion

exchange mechanism between the biomaterial and the physiologic solution. The first step [10, 24] involved is the exchange between Na^+ ions present in a titanate phase on the surface of the biomaterial and H_3O^+ ions coming from the solution, with the formation of negatively charged Ti-OH groups. The second step consists in the interaction with Ca^{++} ions with the formation of positively charged calcium titanate. At last calcium titanate adsorbs phosphate ions and the apatite starts nucleating and growing. They underlined that in natural biomineralization systems, nano-sized spaces of inorganic matrix with special negative charge distributions are usually necessary for the nucleation of apatite [25]. So apatite inducers may be those materials that possess and/or develop both microporous layer and negatively charged surfaces presenting abundant OH groups in SBF [26]. The titania surface contains bridged OH strongly polarized and they are expected to be acidic and exchangeable with cations [27].

On the other hand Oshida [28] reported the formation, on alkali etched pure titanium and Ti-6Al-4V alloy, of rutile mixed with anatase and/or brookite crystalline structures, without any evidence of titanate phase. So the reproducibility of the titanate phase formation during alkali etching is not a univocal effect. Other authors [29, 30] reported data on the bioactive behaviour of simply air heat-treated or H_2O_2/HCl treated titanium samples, presenting anatase on the surface, without Na^+ ions or titanate phase. Furthermore these authors underlined that the in-vitro apatite precipitation was not completely reproducible. Different authors reported also bioactive behaviour of anatase prepared via sol-gel [31–33]. It was also evidenced that amorphous titania or sodium titanate via sol-gel, both in the crystalline or amorphous state, were not bioactive and that the crystallographic structure of anatase was essential at this regard [34]. So it can be concluded that the need of a sodium titanate phase or of the anatase structure on the surface, in order to obtain a bioactive behaviour, can be discussed. It was also claimed that increasing amount of rutile corresponds to deterioration of the bioactivity [35].

Our results confirm that the presence of a titanate phase is not essential in order to obtain a surface able to interact with the physiological solution and that the surface crystallographic structure is quite sensitive to thermochemical treatments conditions. Future work will be performed in order to quantify the Ti-OH groups present, after immersion in physiological solution, on the surfaces prepared and modified during this research activity, because of the importance, as previously reported, of this topic respect to bioactive ability of a material.

By observing our AES data and comparing them with literature ones, it can be concluded that the novel processes proposed (BPAA, BPAV) induce the formation of a graded surface presenting an oxide layer bonded to the bulk through a diffusion region without a net interface. The thickness of the oxide layer due to all the thermochemical treatments is higher than that of the native oxide. In details it can be observed that it is higher in the case of BPAA process respect to BPAV one. The absence of a marked gradient concentration could be a consequence of the passivation treatment performed before alkali etching. On the other hand by using literature process a net interface between the surface layer and the bulk is evident. The increase of thickness of the oxide layer, due to the thermo-chemical treatments, could be potentially beneficial considering that quantitative histomorphometrical data in literature indicated stronger bone tissue reactions to implants with a thick oxide (600–1000 nm) compared to implants with a reduced oxide thickness (17 nm) [22, 36–38]. On the other hand a smooth interface can enhance the adhesion of the surface layer to the substrate.

By observing scratch morphology it can be concluded that the surface layers of the treated materials do not detach in a brittle way. The chemical treated material, without heat treatment, shows a soft and ductile behaviour, while the heat treatment increases the hardness of the surface layer. By comparing different chemical treatment it can be evidenced that the passivation process, performed before alkali etching, enhances the surface layer adhesion and scratch resistance. Among heat treatments, the vacuum process gives the best results.

A relevant question is related to the influence of the surface morphology, due to blasting and chemical etching, on the mechanical performance of the alloy. Fatigue tests of the device are necessary when applying a new process in medical applications in order to ban the risk of fatigue cracks. The described BPAA and BPAV process result in a 43% lower fatigue strength compare to the grit blasted surface of the Ti-6Al-7Nb alloy. This can be related to the fact that the macro roughness of the grit blasted surface is affected by the alkali treatment, which resulted in a small-scale porosity. Fatigue crack initiation is influenced mainly by surface topography and microstructure [39]. Under cyclic test conditions titanium and its alloy are notch sensitive materials and the fatigue strength may drop up to 70% [40–42]. In our study comparing the BPAA and BPAV groups no difference could be detected. It must be underlined that both treatment are performed at 600 °C so the temperature remains below the β-transus and no microstructure evolution due to thermal treatment was detected by metallographic observation. All the treatments recently proposed in literature in order to obtain a bioactive behaviour of titanium and titanium alloys, cause a relevant enhancement in surface porosity due to chemical etching. These data suggest that the effects of the different treatments on the fatigue resistance of the alloys must be carefully investigated.

Another important aspect is related to metal ion release. The hazardous physiological and cellular effects, due to metal ion release from implants, cover a wide series of topics, as local effects, accumulation in lymph nodes and organs, systemic damages, allergies and long-term hypersensitivity. It was assessed that blasted materials show an increase in metal ion release, despite of their good osteointegration ability and it was also underlined that an eventual coating of plasma sprayed hydroxyapatite is not sufficient to reduce significatively the metal corrosion [43].

The values of Al ions concentration detected in SBF after soaking of the materials investigated during this research are always far below those considered as dangerous for living cells. A value of about 400 μg/l in the culture medium of osteoblasts has cytotoxic effects [44], but this value is two orders of magnitude higher than those we obtained.

About Ti ions [45], concentrations up to 100 μg/l have no toxic effect, and again this value is two orders of magnitude higher than those we obtained, except for BPAA-10 M samples. Actually, even low concentrations of Ti ions can influence the release of some bone-associated cytokines, resulting in the enhancement of bone-resorbing agents with a concomitant inhibition of bone-forming agents. This can induce osteolysis at the interface with the implant, causing the loosening of the prosthesis. A concentration of less than 5 μg/l is enough for this, so the new process with standard parameters remains the best performing one. By comparing our data with the literature ones it can be concluded that both BPAV and BPAA processes are of interest at this regard. In fact the metal ion release is quite low in spite of the high roughness due both to sand-blasting and small-scale porosity of the surface. Also the Al content of the alloy and the presence of amorphous oxide on the surface could be potential detrimental factors, but they actually do not. Moreover ion release is lower than what reported in literature in the case of samples treated by similar process. So it can be concluded that the thickness of the oxide layer, its graded interface with the substrate and its crystallographic structure are effective in order to overcome all potential troubles and disadvantages related to ion release.

5. Conclusions

In this paper were reported several characterization data of Ti-6Al-7Nb alloy treated by two innovative treatments, constituted by blasting, passivation, alkali etching and air (BPAA) or vacuum (BPAV) heat treatment. The surface of treated samples shows chemical, structural and morphological modifications. It consists of a layer, free from cracks, presenting a macroscopic roughness due to blasting and a submicrometric porosity due to the chemical etching. The passivation pretreatment causes the formation of different crystallographic phases and of a smoother interface with the substrate. The treated samples evidenced a quite low metal ion release and interact with SBF solution, showing a moderate bioactivity. The disadvantage of theses processes is the decrease in fatigue strength. This aspect suggests that when surface etching and modifications are performed with the aim of enhancing metal osteointegration ability, a careful investigation of their influence on the fatigue resistance must be performed.

Acknowledgments

The Synos Foundation is kindly acknowledged for the research grant supplied. The Centerpulse Orthopaedics is kindly acknowledged for the material support.

References

1. A. GÖRANSSON, E. JANSSON, P. TENGVALL and A. WENNERBERG, *Biomat.* **24** (2003) 197.
2. D. A. PULEO and A. NANCI, *ibid.* **20** (1999) 2311.
3. K. ANSELME, P. LINEZ, M. BIGERELLE, D. LEMAGUER, A. LEMAGUER, P. HARDOUIN, H. F. HILDEBRAND, A. IOST and J. M. LEROY, *ibid.* **21** (2000) 1567.
4. H. DONG and X. Y. LI, *Mat. Sci. Eng.* **A280** (2000) 303.
5. T. KOKUBO, F. MIYAJI, H.-M. KIM and T. J. NAKAMURA, *Amer. Ceram. Soc.* **79** (1996) 1127.
6. H. M. KIM, F. MIYAJI, T. KOKUBO and T. J. NAKAMURA, *Biomed. Mat. Res.* **38** (1997) 121.
7. H. M. KIM, F. MIYAJI, T. KOKUBO, C. OHTSUKI and T. J. NAKAMURA, *Amer. Ceram. Soc.* **78** (1995) 2405.
8. H. M. KIM, F. MIYAJI, T. KOKUBO and T. J. NAKAMURA, *Biomed. Mat. Res.* **32** (1996) 409.
9. H. M. KIM, F. MIYAJI, T. KOKUBO, S. NISHIGUCHI and T. J. NAKAMURA, *ibid.* **45** (1999) 100.
10. H. TAKADAMA, H.-M. KIM, T. KOKUBO and T. J. NAKAMURA, *ibid.* **55** (2001) 185.
11. T. KOKUBO, H.-M. KIM and M. KAWASHITA, *Biomat.* **24** (2003) 2161.
12. X. LU and Y. LENG, *ibid.* **25** (2004) 1779.
13. H. TAKADAMA, H.-M. KIM, T. KOKUBO and T. J. NAKAMURA, *Biomed. Mat. Res.* **57** (2001) 441.
14. H.-M. KIM, H. TAKADAMA, T. KOKUBO, S. NISHIGUCHI and T. NAKAMURA, *Biomat.* **21** (2000) 353.
15. T. KOKUBO, H.-M. KIM, S. NISHIGUCHI and T. NAKAMURA, *Key Eng. Mat.* **192** (2001) 3.
16. J. M. FERNANDEZ-PRADAS, M. V. GARCIA-CUENCA, L. CLERIES, G. SARDIN and J. L. MORENZA, *Appl. Surf. Sci.* **195** (2002) 31.
17. J. M. FERNANDEZ-PRADAS, L. CLÈRIES, E. MARTINEZ, G. SARDIN, J. ESTEVE and J. L. MORENZA, *Biomat.* **22** (2001) 2171.
18. J. M. FERNANDEZ-PRADAS, L. CLÈRIES, E. MARTINEZ and J. L. MORENZA, *ibid.* **23** (2002) 1989.
19. M. C. KUO and S. K. YEN, *Mat. Sci. Eng. C* **20** (2002) 153.
20. S. SPRIANO, M. BRONZONI, F. ROSALBINO and E. VERNÈ, submitted to *J. Mater.Sci. Mater. Med.*
21. G. GIAVARESI, M. FINI, A. CIGADA, R. CHIESA, G. RONDELLI, L. RIMONDINI, P. TORRICELLI, N. N. ALDINI and R. GIARDINO, *Biomat.* **24** (2003) 1583.
22. D. MARTINI, M. FINI, M. FRANCHI, V. DEPASQUALE, B. BACCHELLI, M. GAMBERINI, A. TINTI, G. GIAVARESI, V. OTTANI, M. RASPANTI, S. GUIZZARDI and A. RUGGERI, *ibid.* **24** (2003) 1309.
23. F. LIANG, L. ZHOU and K. WANG *Surf. Coat. Tech.* **165** (2003) 133.
24. B. C. YANG, J. WENG, X. D. LI and J. X. D. ZHANG, *Biomed. Mat. Res.* **47** (1999) 213.
25. H. B. WEN, J. G. C. WOLKE, J. R. DE WIJN, Q. LIU and F. Z. CUI, *Biomat.* **18** (1997) 1471.
26. P. LI, C. OHTSUKI, T. KOKUBO, K. NAKANISHI, N. SOGA and K. J. DE GROOT, *Biomed. Mat. Res.* **28** (1994) 7.
27. M. BROWNE and P. J. GREGSON, *Biomat.* **15** (1994) 894.
28. US Patent 6183255.
29. X. X. WANG, S. HAYAKAWA, K. TSURU and A. J. OSAKA, *Biomed Mat. Res.* **54** (2001) 172.
30. *Idem.*, *Biomat.* **23** (2002) 1353.
31. M. WEI, M. UCHIDA, H. M. KIM, T. KOKUBO and T. NAKAMURA, *ibid.* **23** (2002) 167.
32. P. LI, I. KANGASNIEMI, K. DE GROOT and T. J. KOKUBO, *Am Ceram. Soc.* **77** (1994) 1307.
33. P. LI, I. KANGASNIEMI and K. DE GROOT, *Bioceramics* **6** (1993) 41.
34. M. UCHIDA, H. M. KIM, T. KOKUBO and T. J. NAKAMURA, *Am. Ceram. Soc.* **84** (2001) 2969.
35. X. X. WANG, S. HAYAKAWA, K. TSURU and A. OSAKA, *Biomat.* **23** (2002) 1353.
36. Y. T. SUL, C. B. JOHANSSON, K. ROSER and T. ALBREKTSSON, *ibid.* **23** (2002) 1809.

37. M. C. GARCÍA-ALONSO, L. SALDAÑA, G. VALLÉS and J. L. GONZÁLEZ-CARRASCO, *ibid.* **24** (2003) 19.
38. D. ZAFFE, C. BERTOLDI and U. CONSOLO, *ibid.* **24** (2003) 1093.
39. J. L. GILBERT and H. P. PIEHLER, *Metall. Trans.* A **20A** (1989) 1715.
40. S. YUE, R. M. PILLAR and G. C. J. WEATHERLY, *Biomed. Mat. Res.* **18** (1984) 1043.
41. M. WINDLER and R. KLABUNDE, "Titanium in Medicine," edited by D. M. Brunette, P. Tengvall, M. Textor and P. Thomas, (Springer Verlag Berlin Heidelberg New York, 2001).
42. S. D. COOK, N. THONGPREDA, R. C. ANDERSON and JR R. J. J. HADDAD, *Biomed. Mat. Res.* **22** (1988) 287.
43. M. BROWNE and P. J. GREGSON, *Biomat.* **21** (2000) 385.
44. Y. OKAZAKI, S. RAO, Y. ITO and T. TATEISHI, *ibid.* **19** (1998) 1197.
45. J. Y. WANG, B. H. WICKLUND, R. B. GUSTILO and D. T. TSUKAYAMA, *ibid.* **17** (1996) 2233.

Received 3 May
and accepted 17 November 2004